The calibration challenge when inferring longitudinal track profile from the inertial response of an in-service train

Paraic Quirke[a,1], Eugene J. OBrien[b,2], Cathal Bowe[c,3], Daniel Cantero[d,4], Abdollah Malekjafarian[e,5*]

[a] Murphy Surveys, Global House, Kilcullen Business Park, Kilcullen, Co. Kildare, Ireland
[b] School of Civil Engineering, University College Dublin, Dublin D04T3F9, Ireland.
[c] Iarnród Éireann Irish Rail, Technical Department, Engineering & New Works, Inchicore, Dublin 8, Ireland.
[d] Department of Structural Engineering, Norwegian University of Science & Technology, Trondheim, Norway.
[e] Structural Dynamics and Assessment Laboratory, School of Civil Engineering, University College Dublin, Dublin D04T3F9, Ireland.

email: [1]paraic.quirke@gmail.com, [2]eugene.obrien@ucd.ie, [3]cathal.bowe@irishrail.ie, [4]daniel.cantero@ntnu.no, [5]abdollah.malekjafarian@ucd.ie

[*]Corresponding author

ABSTRACT: An Irish Rail intercity train was instrumented for a period of one month with inertial sensors. In this paper, a novel calibration algorithm is proposed to determine, with reasonable accuracy, vehicle model parameters from the measured vehicle response data. Frequency domain decomposition (FDD) is used to find the dominant frequencies in the captured data. Randomly chosen 2 km data segments are chosen from a number of datasets, thereby averaging out the effects of variations in track longitudinal profile, track stiffness, signal noise and other unknowns. The remaining dominant peaks are taken to be vehicle frequencies. An optimisation technique known as Cross Entropy is used to find vehicle mass and stiffness properties that best match modal vehicle eigenfrequencies identified in the frequency analysis. Finally, the calibrated vehicle is run over a measured track profile and the resulting model output is compared to measured data to validate the results.

Keywords: Calibration; Measurement; Frequency Domain Decomposition; Railway Vehicle Dynamics; Cross Entropy; Optimisation.

1. INTRODUCTION

Measurement of the inertial response of in-service trains has the potential to provide real-time railway track condition information to owners of the track asset. The increase in the frequency of measurement provided by using in-service trains can aid maintenance planning and reduce the cost of repair through timely intervention. As a result, there is increased interest in this area of research recently

(Malekjafarian et al. 2019; Weston et al. 2015). Xiao et al. (2020) proposed a Kalman filter algorithm for identifying railway track profile using vehicle dynamic responses. De Rosa et al. (2019) employed vehicle responses in the time and frequency domains to estimate the lateral and cross alignment in a railway track.

Numerical models are used to predict the interaction between the vehicle, railway track and bridges to investigate a variety of problems (Malekjafarian et al. 2017). Zhai et al. (2009) give fundamentals on the topic while Lou (2007) presents a complete analytical description of a 2D model using finite elements. Other authors use the same 2D numerical model to investigate ground vibrations (Francois et al. 2012; Kouroussis and Verlinden 2013) and bridge response under dynamic load (Azimi 2011). In the technique presented by OBrien et al. (2017), it is hypothesised that numerical vehicle models can be used in an inverse technique to find track profile. The simulated 'measured' response of a railway vehicle is used as input to an optimisation technique where a track longitudinal profile is inferred by finding output from the numerical vehicle model that best fits the measured data. The actual track profile can be inferred through this technique, enabling fault detection through comparison with the past profile. It is also hypothesised that this method can be used to find railway bridge damage (Quirke 2017). A new Kalman filter algorithm is proposed by Xiao et al. (2020) to identify the track irregularities of railway bridges using responses measured on in-service trains. The model includes bridges as the high-speed rail lines in China mainly consist of bridges. Xu et al. (2020) developed a fully coupled model for vehicle-track-subgrade interaction where the system interactions are simultaneously deliberated and solved using mathematical matrix formulations. They have improved the computational stability and infinite-length-computation problem with their model.

To enable these methods in practice, accurate calibration of a numerical vehicle model representing the in-service train is required. Several researchers (Xu and Zhai 2019a, 2019b; Zhai et al. 2013a; Zhai et al. 2013b) have developed 3D numerical models in recent years. Using 3D models seems to be required when the problem of train track bridge interaction is investigated. However, when only train track interaction is considered, use of a 2D model reduces the computational effort involved in executing the thousands of simulations required to return an inferred profile. Nguyen et al. (2014) compare the

dynamic responses for both 2D and 3D models and conclude that the 2D vehicle response provides a 'sufficiently accurate assessment' of the vertical response in the 3D model. In practice, numerical models are generally created using theoretical values for properties which are often unconfirmed in reality. Numerical models should be, in so far as possible, a true representation of how mass, stiffness and damping are distributed in the physical model and should provide an accurate representation of the physical response of the vehicle and infrastructure (Absi and Mahadevan 2016). Modelling errors can be categorised into three types: a) Model form errors - i.e. due to incorrect assumptions regarding the actual physics of the system, particularly when the response exhibits non-linear behaviour. b) uncertainty in model parameters and c) model order errors as a result of discretisation of complex systems (Mottershead and Friswell 1993). Throughout the literature, linear 2D car models are used to estimate the response of railway vehicles with good comparison to measured responses generally achieved, for instance see (Ferrara 2013; Sun and Dhanasekar 2002). Therefore the multi-body vehicle model appears to satisfy the criteria for a) and b) above. This leaves uncertainty in model parameters as the most likely cause of error in numerical railway vehicle/track models.

In typical vehicle modal identification experiments, particularly in the automotive industry, excitement of the vehicle is achieved by means of a shaker or some other measurable input. The response of the vehicle is measured and, through frequency analysis, the known input is eliminated from consideration. Frequency response functions are employed to identify the modes of the vehicle. It is difficult to use this technique on railway vehicles due to their size and heavy damping properties (Ahmadian 2005). Operational Modal Analysis (OMA) is a modal identification method commonly used in situations where the system input or excitation frequency cannot be determined (L. Zhang et al. 2005). Calibration of railway vehicle properties through experimental measurement is investigated by Ribeiro et al. (2013). Frequencies and mode shapes of 13 vibration modes of an Alfa Pendular railway vehicle are found through dynamic testing. Genetic algorithms are used in an iterative method to determine 17 parameters of a representative 3D numerical vehicle model. Good correlation is found between calibrated model outputs and experimental measurement. The authors use a finite-element vehicle model so that local vibration modes can be identified. Excitation of vibration modes is achieved by means of the impact

loading effect of people jumping in the car body. Li et al. (2007) use the Rao-Blackwellized particle filter method to estimate vehicle parameters to aid condition monitoring. Diana et al. (2002) compare the simulated results of a rigid multi-body vehicle and flexible finite element model before comparing both to measured data. A better match to the finite element model is achieved in the car body and it is concluded that this model type should be considered for the car body when assessing passenger comfort. Bogie flexible modes were found above 25 Hz. Non-contact laser vibrometers are used in another study to determine car body bending modes using a 1/10th scale model of a metro vehicle (S. Popprath et al. 2006). Ahmadian (2005) uses both peak-picking and Frequency Domain Decomposition (FDD) to identify rigid and flexible car body vibration modes in the 0–10 Hz range using measured data from 20 accelerometers. Stribersky et al. (2002) use experimental modal analysis to validate a virtual vehicle system, achieving good agreement between measured and simulated data. However, there is a significant challenge where the train is not available for full experimental testing and only the data measured from the train running on track is available for calibration. This is illustrated in Figure 1.
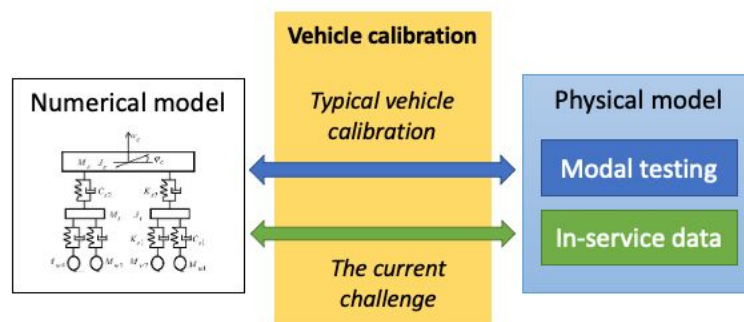

Figure 1. The research gap addressed in this paper.

This paper presents a novel method whereby the measured inertial response of a railway vehicle can be used, with prior knowledge of some vehicle mechanical properties, to calibrate a 2D numerical vehicle model. In this case, due to operational requirements the train was not made available for sufficient time to conduct a full experimental modal analysis, meaning OMA was required for calibration. Budget constraints and limitations on possible sensor locations limited the scope of the testing and the number of sensors used. To address these issues, a new method is proposed using an adapted FDD technique to identify dominant frequencies in the measured train data. A numerical model of train track interaction

is developed using the finite element method. An in-service train was instrumented using several inertial sensors. The train measurements were recorded over a period of two month when the train was in service between Dublin and Belfast. A large data set including the in-service measurements was used to calibrate the train numerical model. It is assumed that by analysing a large amount of data from different sections of track, the effect of variability in vehicle speed and variation in track profile and track stiffness is averaged out and the vehicle frequencies begin to dominate the frequency spectrum. The use of a large number of datasets also reduces the effect of signal noise. Several data samples are selected from the data set and subjected to a filtering process. Then, the proposed FDD algorithm is used for vehicle frequency identification. Cross Entropy (CE) optimisation (Rubinstein and Kroese 2013) is employed to find the vehicle properties following frequency identification. This algorithm is chosen due its robustness when solving multi-variate problems and its insensitivity to local minima. CE uses Monte Carlo simulation to generate a population of trial solutions from a mean and standard deviation for each variable being sought. Finally, the proposed algorithm is validated by comparing the recorded data to those generated using the calibrated model.

The paper is structured as follows. Firstly, the 2D car vehicle model used in modal analysis and in the validation is described in section 2. A description of the field testing and measurement apparatus is given in section 3. Following this, some samples of the raw data, frequency analysis and justification of filtering techniques used to de-noise the data are presented in section 4. Vehicle frequency identification through FDD analysis and results are presented in section 5. Next, using the identified vehicle frequencies, the results of a Cross Entropy optimisation to identify matching 2D vehicle model eigenfrequencies is presented in section 6. Finally, in section 7 the outputs of a simulation where the calibrated vehicle is run over a measured track are compared to measured data.

2. MODEL DESCRIPTION

A 2D car model, shown in Figure 2, is used in the calibration process to find vehicle eigenfrequencies which match observed frequencies in the measured data. Following calibration, the model is run over a section of track with a measured profile, the outputs of which are compared to the measured data in order to validate the model. The main car body is represented by a rigid bar with mass, m_v, and mass

moment of inertia, J_v. Similarly, the two vehicle bogies are modelled as rigid bars with masses (m_{b1}, m_{b2}) and mass moments of inertia (J_{b1}, J_{b2}). Bogie connections are located L_{v1} and L_{v2} from the car body centre of mass for bogie 1 and bogie 2 respectively. The vehicle axles are modelled as point masses ($m_{w1}, m_{w2}, m_{w3}, m_{w4}$) and are spaced at L_{b1} and L_{b2} apart for bogie 1 and bogie 2 respectively. Primary and secondary suspension systems are represented by springs (k_p, k_s) and dampers (c_p, c_s). Nonlinearities are not considered in either suspension system.
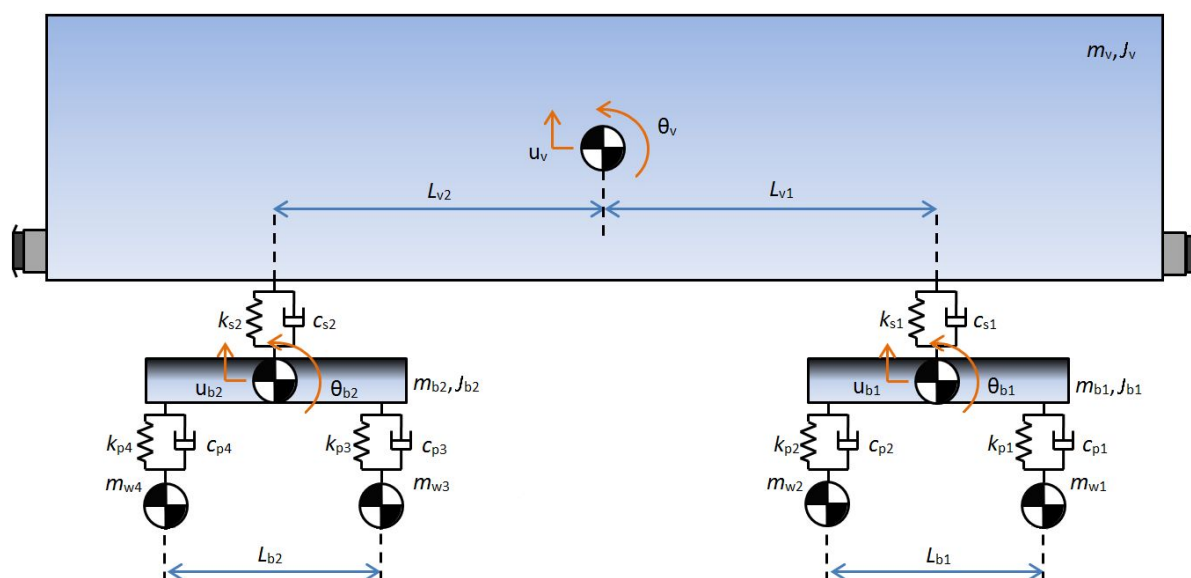

Figure 2. 2D Car model.

The model has 10 degrees-of-freedom (DOF); however, when the vehicle is coupled to the track, the axle masses are rigidly connected to the DOF of the rail (Lin and Trethewey 1990). This method of coupling leaves 6 vehicle DOF to be considered: vertical translation, u_v, and rotation, θ_v, of the car body and vertical translation (u_{b1}, u_{b2}) and rotation (θ_{b1}, θ_{b2}) of the two individual bogies. Each of these DOFs has an associated mode of vibration: car body bounce, car body pitch, bogie bounce and bogie pitch. More detailed descriptions of the vehicle model, including equations of motion and model matrices, can be found in the following texts (Azimi 2011; Lei and Noda 2002; Sun and Dhanasekar 2002).

Vehicle model eigenfrequencies are determined by calculation of eigenvalues and eigenvectors through modal analysis of the vehicle mass and stiffness matrices. Due to similarities in the mass and stiffness

properties of the bogies, it is assumed that the model can be accurately described by 4 eigenfrequencies: bounce and pitch of both the car body and the bogie.

3. DESCRIPTION OF TEST

In December 2015 Irish Rail procured the installation of sensors on a Hyundai-Rotem InterCity fleet car 22337. Set 37, a 5-car train set, was chosen as it was configured to run in both the Republic of Ireland and Northern Ireland Railways. This configuration setting meant that the train would remain on the Dublin-Belfast line until its next maintenance examination, providing the maximum repeatability possible for the short duration of the test.

The sensor locations are shown in Figure 3. The sensors were attached to the trailer (non-powered) bogie to avoid contamination of signals with noise due to frequencies associated with the power train. A tri-axial accelerometer and tri-axial gyrometer were attached to the Electronic Train Protection and Warning System (E-TPWS) unit, the closest possible mounting location to the centre of gravity of the bogie frame (see Figure 4(a)). The inertial measurement unit used to record the bogie angular velocity was capable of measuring accelerations but an additional accelerometer was actually used to record the accelerations.

A uniaxial accelerometer, measuring vibration in the vertical direction, was placed on the underside of each axle box, in line with the centreline of the axle (See Figure 4(b)). The properties of all sensors used in the test are provided in Table 1. The system sampling frequency was variable but set to 500 Hz for the majority of the testing.
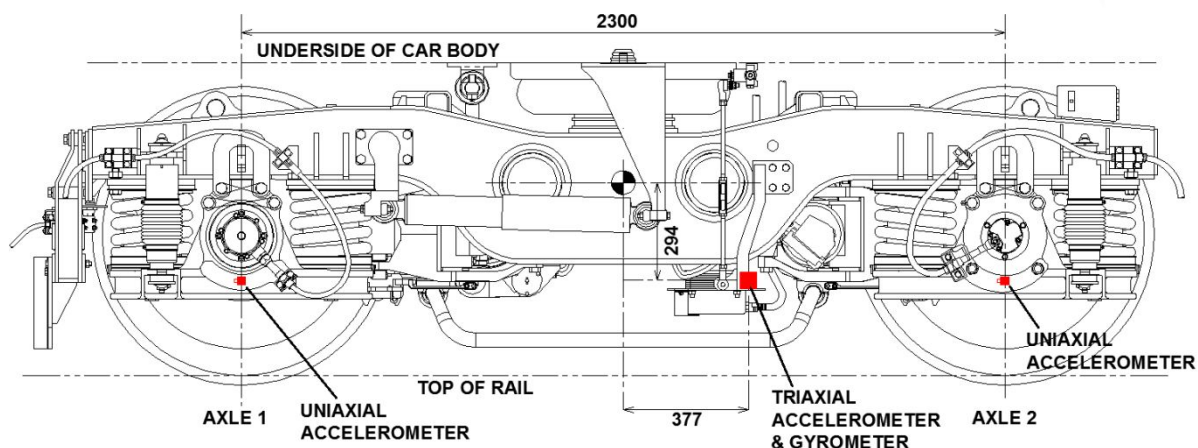
Figure 3. Sensor installation locations on trailer bogie (dimensions in mm). (CAD drawing sourced from Tokyu Car Corporation).

Table 1. Properties of sensors

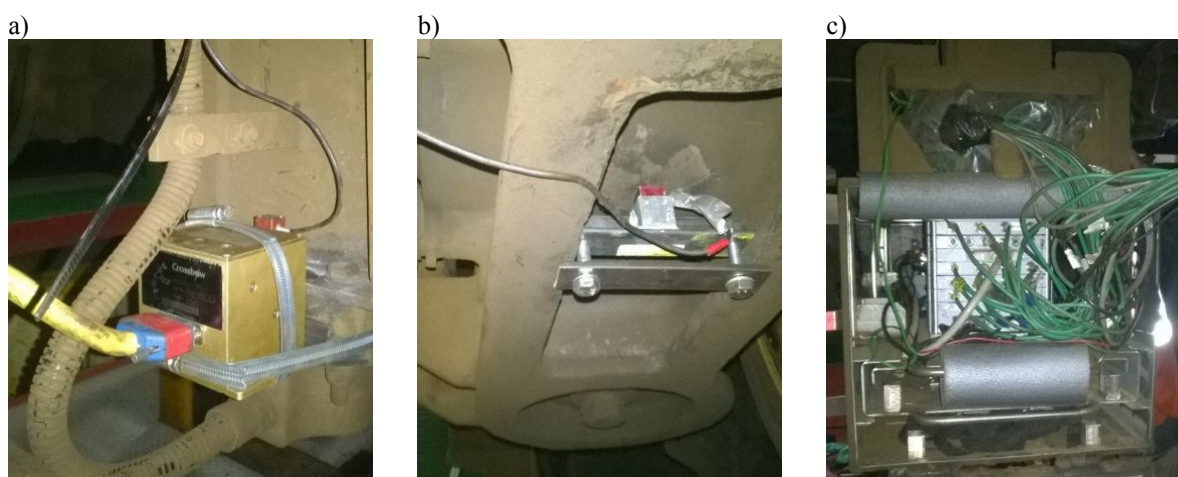| Sensor Location	Type	Name	Range
Axle box – Bounce	Uniaxial Accelerometer	Disynet-DA2201-050g	±50 g
Bogie – Bounce	Triaxial Accelerometer	Disynet-DA3802-015g	±15 g
Bogie – Pitch	Triaxial Gyrometer	Crossbow VG400CC-200	±200 °/s

a)　　　　　　　　　　b)　　　　　　　　　　c)

Figure 4. a) Bogie mounted gyrometer and accelerometer; b) Uniaxial accelerometer clamped to axle box; c) Data logger (HBM Somat eDAQ lite) housed in disused train coupler box in close proximity to sensors

The system power supply was taken from a spare circuit breaker on the train, avoiding the need for batteries. A back-up battery was provided to ensure the system remained in stand-by mode if the main train power was switched off. A Global Positioning System (GPS) antenna recorded the vehicle position at a sampling frequency of 5 Hz.

The system was configured to begin recording once train movement was detected by the GPS. The data was collected and stored in a HBM Somat eDAQ-lite data logger located in a disused coupler box underneath the train in close proximity to the trailer bogie (see Figure 4(c)). The logger was capable of

storing 32GB of data with the aid of an external storage system. A secure Wi-Fi router enabled operators to sit on board and download recorded data from the eDAQ on a weekly basis. Testing was carried out on the Dublin-Belfast line from 13 January to 3 February, 2016. The trainset made 57 journeys on the line during this period. The Irish Rail network is measured in miles and yards however, distances are presented in km throughout this paper. A conversion factor of 1 mile = 1.60934 km can be used if required.

4. SAMPLE DATA AND FILTERING

In this section samples of raw data are presented in the time domain and analysed in the frequency domain to determine the appropriate filtering actions required prior to FDD analysis. A sample of an unfiltered bogie angular velocity signal is shown in Figure 5(a). There is clearly an offset and drift in the raw signal as it does not oscillate about 0 as expected. This problem may be associated with temperature changes due to the exposed siting of the sensor (Weston et al. 2015). In addition, an issue with the sensor calibration arising from the offset of the sensor from the bogie pivot point was identified post-measurement. A 6th order Butterworth high-pass filter is applied to remove content below 0.25 Hz, thereby removing this drift. In addition, a calibration factor of 23.9, determined through a post-measurement calibration test, is applied to the data to account for the offset from the bogie centre of mass. The measured output is converted from °/s to rad/s to match numerical model units for comparison to numerical model output as detailed in section 7. On the other hand, the recorded vertical acceleration signals provided reliable and correct response. A sample of the raw data is given in Figure 6(a).
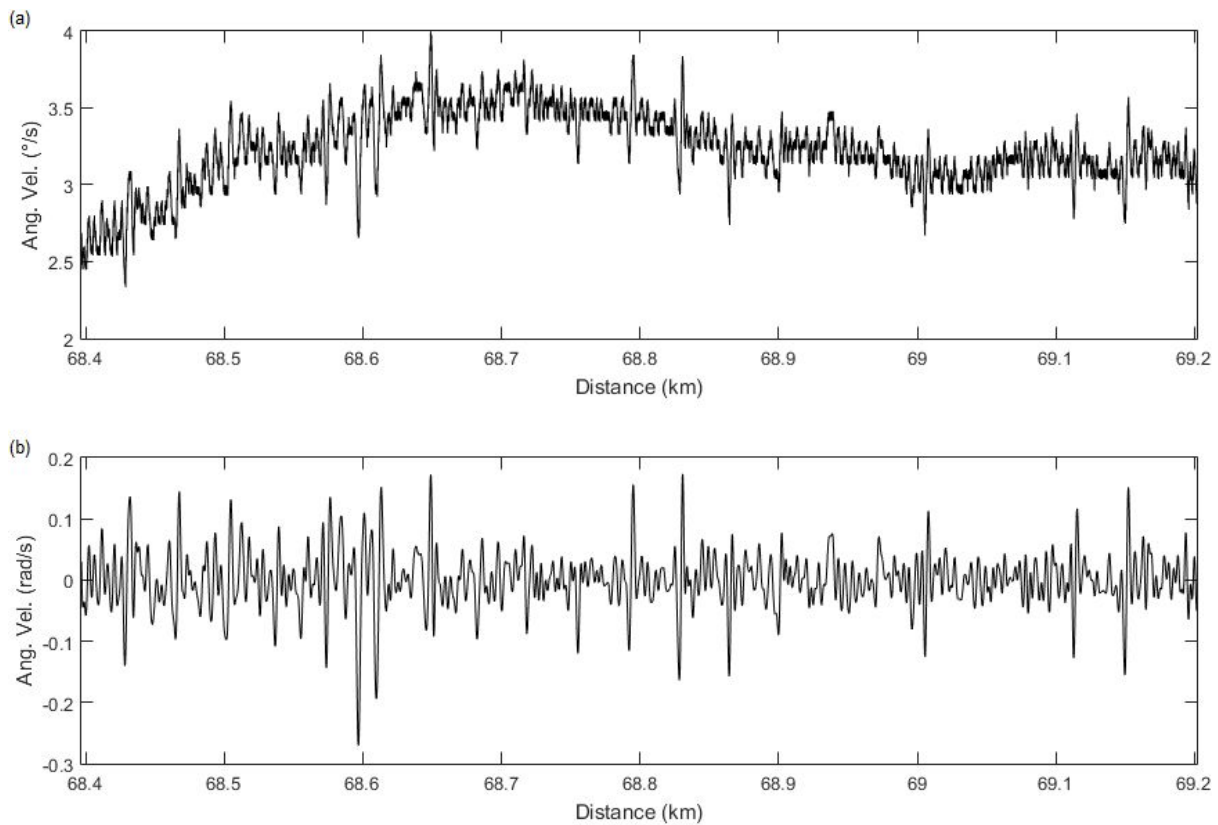
Figure 5. Bogie angular velocity signal (pitch velocity) as a function of distance from the start point (Dublin); a) Unfiltered signal; b) Band-pass filtered signal (0.25-25 Hz)
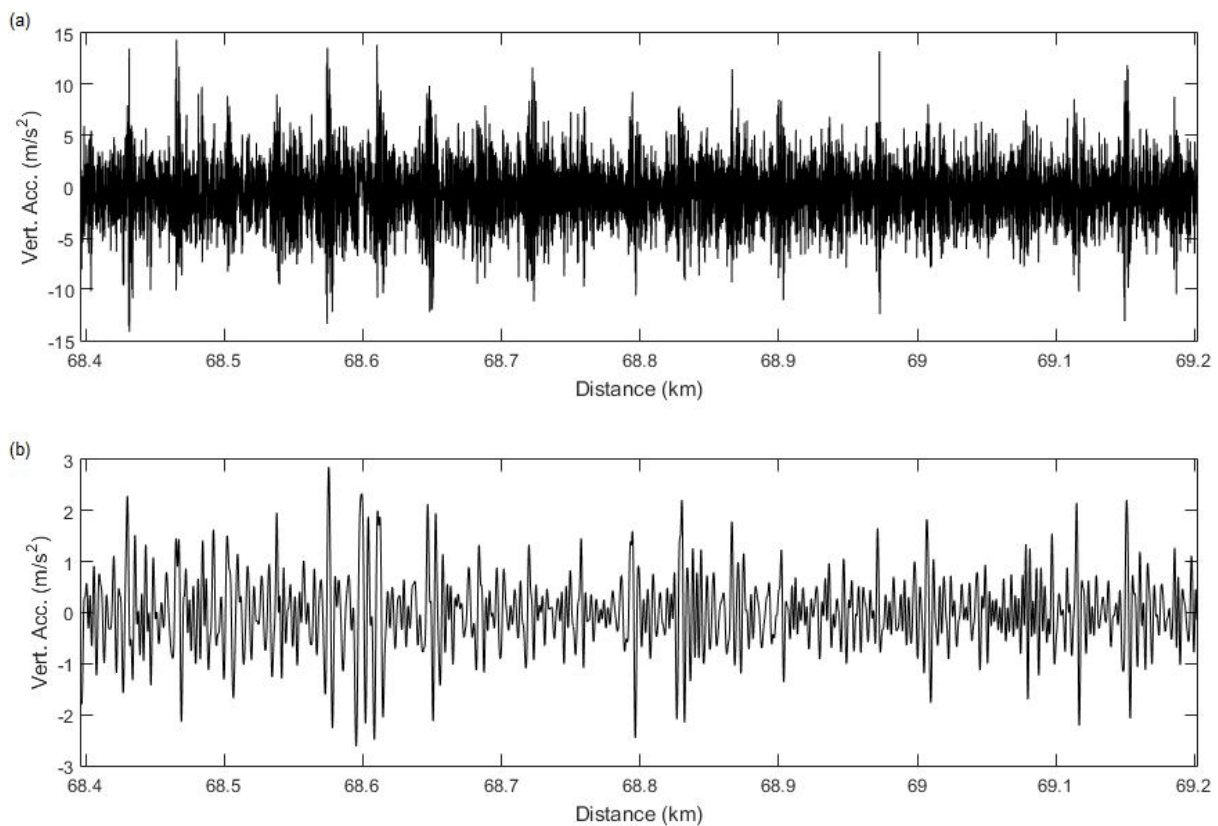

Figure 6. Bogie vertical acceleration signal as a function of distance from the start point (Dublin); a) Unfiltered signal; b) Band-pass filtered signal (0.25-25 Hz)

The power spectral densities (PSD) of a number of signals are shown in Figure 7. Three datasets are chosen through the track section between 68.4 km and 69.2 km. Datasets with distinct differences in vehicle mean forward velocity are chosen in order to separate out frequencies in the data related to this parameter. In Figure 7(a) it can be observed that a frequency of 77.64 Hz exists in all 3 datasets, meaning that data contained within the signal at this frequency is independent of vehicle velocity. This frequency may be associated with the Electronic Train Protection and Warning System (E-TPWS) receiver to which the gyrometer was attached.

Figure 7(b) shows the PSD of three samples of bogie vertical acceleration for varying vehicle forward velocity. A detailed view of the results between 45 Hz and 60 Hz is shown in Figure 7(c). It can be observed that the dominant frequency in the 3 datasets increases from 50.29-57.62 Hz. These frequencies are clearly dependent on vehicle forward velocity as the peaks are different for each speed. These dominant peaks are associated with the frequency of track sleeper spacing. Irish Rail prefabricate 39 m track panels with sleepers spaced at 0.7 m centres. The welds joining these panels introduce imperfections in the rail and this can be observed as regular spikes in the raw data. It is observed that there is low power in the 25–50 Hz region of both spectra.

From the literature, typical vehicle eigenfrequencies range from 0.5–15 Hz. Therefore a 6th order Butterworth bandpass filter (0.25–25 Hz) is applied to all data channels prior to FDD analysis. The chosen band retains the frequencies of interest, removes drift/error, the influence of the track sleeper spacing and other unwanted noise. Examples of filtered signals for bogie angular velocity and vertical acceleration are shown in Figure 5(b) andFigure 6(b) respectively.
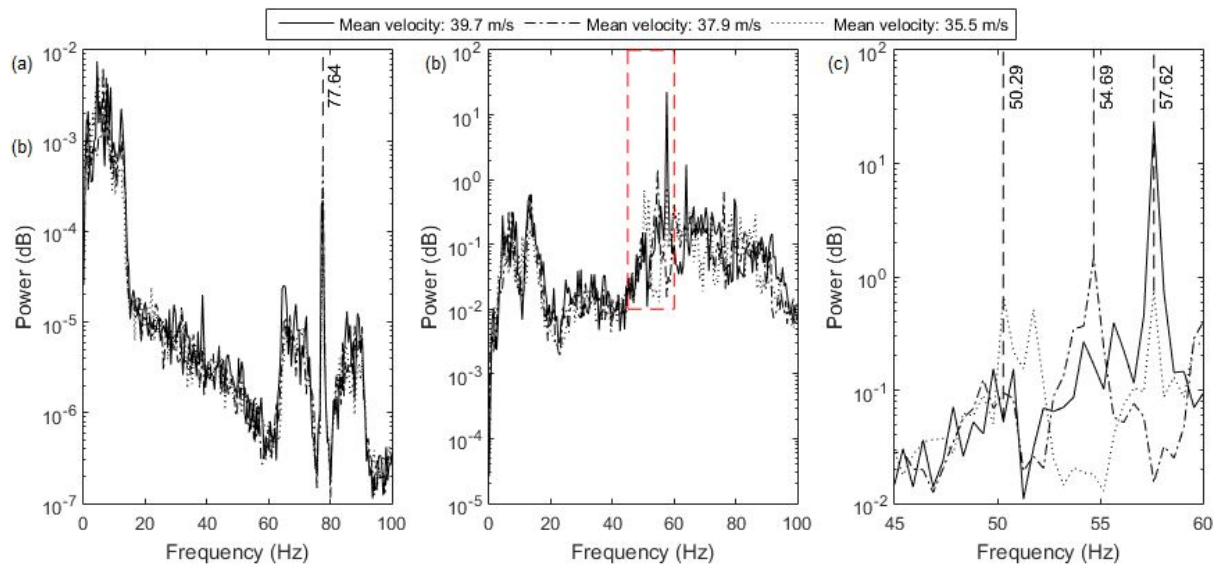
Figure 7. Power spectral density of captured signals. a) Bogie angular velocity 0–100 Hz; b) Bogie vertical acceleration 0–100 Hz; c) Detailed view of bogie vertical acceleration 45–60 Hz.

5.　VEHICLE FREQUENCY IDENTIFICATION

Following the filtering process, a frequency analysis is carried out to determine the dominant vehicle frequencies. Frequency domain decomposition is an OMA technique used to identify modal parameters (natural frequencies and mode shapes) of a structure from measured responses which are typically recorded at several locations on the structure at the same time (see Figure 8(a)) (Brincker et al. 2001). Sensors are typically placed in pre-determined locations to identify the mode shapes of the structure. It applies singular value decomposition (SVD) to the power spectral density (PSD) matrix of the measured responses (Malekjafarian and OBrien 2014). If applied to measured output from a bridge for example, stochastic excitations due to traffic loading or wind are filtered out and frequencies associated with the bridge, common to all data segments, are identified.

When applied to data measured on the bogie of an in-service train, the section of data chosen for analysis is associated with a section of track. In this case the influence of the track is not random and has an influence on all data channels. Therefore frequencies associated with the track may obscure the frequencies associated with the vehicle which are typically in the same range. In addition, as the forward velocity of the vehicle changes, the vehicle will be excited at different frequencies.

Typical 2D vehicle model eigenfrequencies are listed in Table 2, calculated by applying modal analysis using published vehicle properties for a variety of 2D vehicle models found in the literature. Most

vehicle types found are either locomotives or unpowered coaches. No 2D vehicle model information for a diesel multiple unit similar to the Irish Rail 22000 train could be found. It can be observed that the typical frequencies for the vehicle modes of vibration range between 0.52–1.36 Hz for car body bounce, 0.67–2.07 Hz for car body pitch, 3.85–8.55 Hz for bogie bounce and 3.38–12.50 Hz for bogie pitch.

Table 2. Eigenfrequencies of 2D railway vehicle models (in Hz)

Vehicle	Source	Body Bounce	Body Pitch	Bogie Bounce	Bogie Pitch
ETR500Y Locomotive	Liu et al. (2009)	0.65	0.72	4.83	5.91
ETR500Y Coach	Liu et al. (2009)	0.52	0.67	3.85	6.07
Eurostar	Kouroussis et al. (2011)	1.36	2.07	8.55	12.50
ICE2 Locomotive	Domenech et al. (2014)	1.21	1.48	6.59	5.01
ICE2 Coach	Domenech et al. (2014)	0.67	0.81	5.84	8.31
Manchester Benchmark	Iwnick (1998)	1.07	1.28	7.47	11.68
Pioneer – R	Antolin et al. (2013)	0.63	0.72	4.57	5.71
Pioneer – M	Antolin et al. (2013)	0.69	1.24	3.94	3.38
Shinkansen	Lin et al. (2005)	0.76	1.03	6.62	8.27
TGV	Lin et al. (2005)	0.74	1.22	6.74	8.20
Unidentified	Diana et al. (2002)	1.02	1.38	5.71	9.07

The method employed to determine vehicle eigenfrequencies from the measured data, is a type of 'segmental' FDD, where input data is sampled from different sections of track and from multiple datasets. This random selection method is illustrated in Figure 8(b). Track profile, stiffness and vehicle speed will vary in the different data segments allowing the vehicle frequencies to dominate the frequency spectrum. Singular values output from the FDD analysis can therefore be more confidently associated with the vehicle.
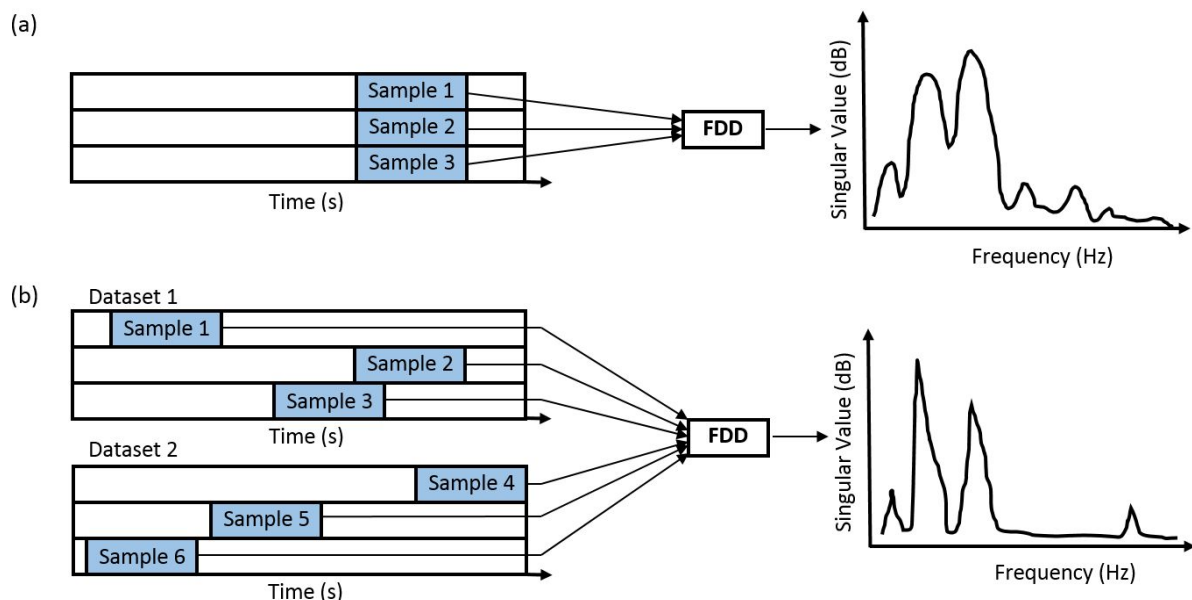

Figure 8. FDD Methodology; a) Traditional FDD: data sampled over same time period from a number of channels; b) Segmental FDD: data sampled randomly from multiple datasets, in this case multiple train trips.

This segmental FDD method is used here to identify vehicle eigenfrequencies. The signal samples, each 2 km in length, are randomly selected from 30 datasets. It was not recorded whether these segments were from straight or curved sections of track. Given this uncertainty, it is important to note that the

approach may not work well when track is curved. Each dataset contains six measured output channels giving the response of the vehicle bogie and axles over a 90 km section of the Dublin-Belfast railway line. The analysis is repeated a number of times for each mode of interest. The results of the FDDs are then summed, further filtering out frequencies not associated with the vehicle. The number of FFD results used in each analysis are listed in Table 3.

Table 3. Number of FDD results used in analysis

Analysis	No. of Sensors	No. of FDDs Summed
Axle 1 Bounce	2	20
Axle 2 Bounce	2	20
Bogie Bounce	1	50
Bogie Pitch	1	50
System (All Bounce)	5	20

Singular values for the frequency range of interest produced from FDD analysis of vertical acceleration measured on axle 1 and axle 2, are shown in Figure 9(a) and (b) respectively. The dominant frequencies in these spectra are 7.46 Hz for axle 1 and 7.71 Hz for axle 2. Both of these frequencies can be found across a plateau in the bogie vertical acceleration singular values shown in Figure 9(c). A dominant peak of 6.53 Hz remains when the frequencies associated with axle bounce are not considered. There is also a significant peak occurring at 5.45 Hz.

Singular values for bogie angular velocity about the Y-axis (pitching) is shown in Figure 9(d). There is a dominant peak occurring at 4.31 Hz. The bogie rigid pitch mode is expected to be present in the accelerometer bounce spectrum due to the offset of the sensor from the bogie centre of gravity. Additional frequencies may be due to flexible bending modes in the bogie frame itself however it is impossible to confirm this without the installation of additional sensors.
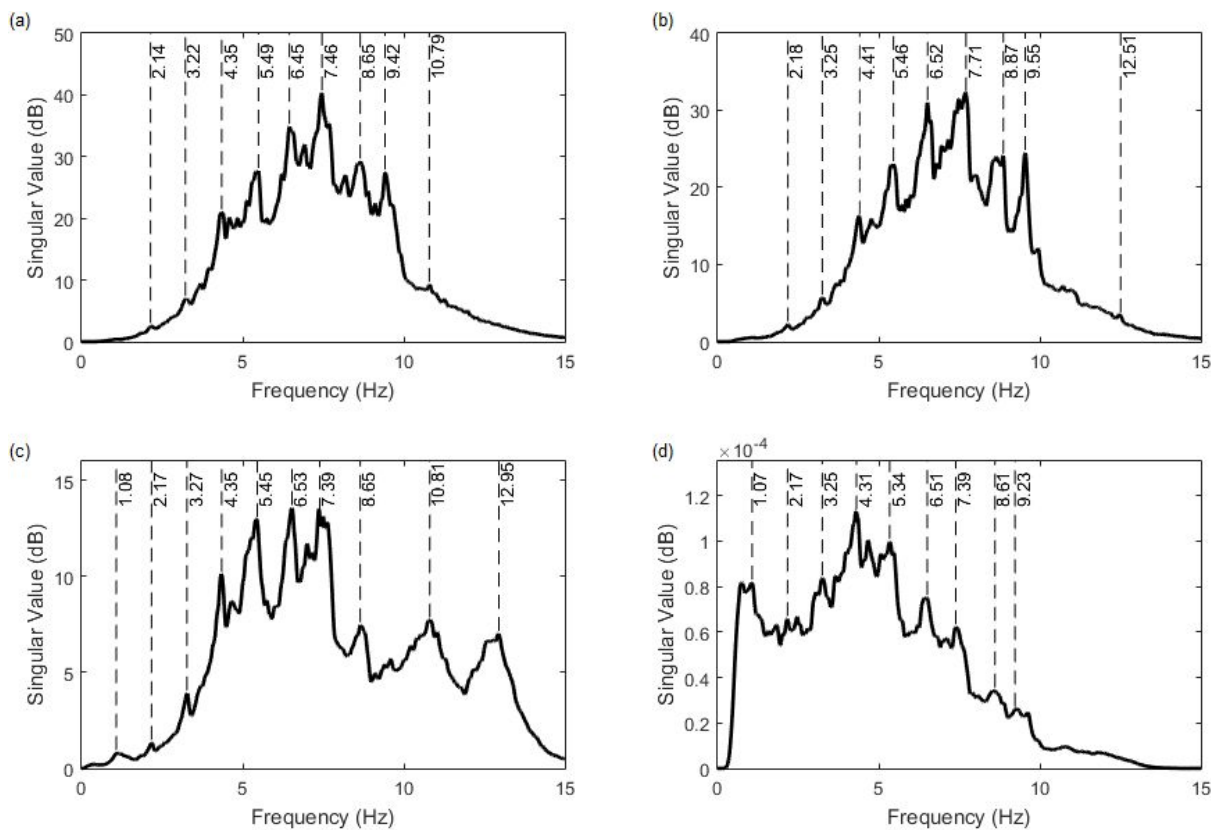
Figure 9. Sum of singular values from FDD analysis of 30 datasets (2 km signal segments). a) Axle 1 vertical acceleration; b) Axle 2 vertical acceleration; c) Bogie vertical acceleration; d) Bogie angular velocity.

The frequencies identified as being the most likely to be related to the vehicle and their specific modes are summarised in Table 4. It is assumed that these dominant frequencies are the rigid body vibration modes of the vehicle. These values are used as target frequencies to find vehicle parameters that return a 2D numerical model with matching eigenfrequencies.

Table 4. Summary of dominant vehicle frequencies

Mode	Frequency (Hz)
Car Body Bounce	1.08
Car Body Pitch	2.19
Bogie Bounce	6.53
Bogie Pitch	4.31

6. DETERMINATION OF VEHICLE PARAMETERS FOR 2D MODEL

6.1 *Vehicle properties from train manufacturer*

As described in Section 3, inertial sensors were attached to the bogie of an in-service Irish Rail train, a Hyundai-Rotem 22000 series vehicle. A selection of vehicle properties are known to be within certain ranges following analysis of information gathered from the vehicle manufacturer. These properties

include vehicle body mass (which can vary due to passenger load, fuel tank load, water tank load, and foul tank load), bogie mass, primary suspension properties, secondary suspension properties and some information on primary dampers.

It is acknowledged that properties for the primary dampers appear to be bi-linear, and the stiffness and damping of the air springs comprising the secondary suspension system are highly non-linear in nature. The properties of this active suspension system are varied according to the position of the vehicle main body relative to the bogie frame and air is pumped into or released from the air spring to increase or decrease the internal pressure accordingly.

Due to uncertainty in the values of all stated vehicle properties and the uncertainty in using a 2D model to characterise a 3D vehicle, an optimisation technique is used to find the best-fit properties. Uncertainty in possible property values is varied according to the confidence in the value which is influenced by factors such as its linear or non-linear nature. Upper and lower limits on the parameter trial values are specified to account for this uncertainty and to avoid the generation of unrealistic estimates.

Vehicle properties gathered from manufacturers' drawings and technical specifications are summarised in the tables below. Table 5 provides a breakdown of the assumed contribution of various mass components to the mass of the vehicle car body. There are no records of patronage or tank loading available for the duration of the test. Therefore loading estimates are required within the ranges stated in the table. Manufacturers' values for other required vehicle properties, and ranges based on uncertainty in the values, are listed in Table 6.

Table 5. Mass properties of car body

Contribution	Mass at full capacity (kg)	Range (Low)	Mass (Low) (kg)	Range (High)	Mass (High) (kg)
Tare Load Condition	35 032	-	35 032	-	35 032
Passenger (54 × 80 kg)	4 320	25 %	1 080	75 %	3 240
Wheelchair	300	0 %	-	100 %	300
Luggage	188	25 %	47	75 %	141
Fuel tank	1 612	25 %	403	75 %	1 209
Waste tank	650	25 %	163	75 %	488
Water tank	500	25 %	125	75 %	375
Total	**42 602**		**36 850**		**40 644**

Table 6. Manufacturers' vehicle properties and uncertainty ranges

Component	Value	Range (Low)	Value (Low)	Range (High)	Value (High)
Trailer bogie mass (kg)	3 087	90 %	2 778	125 %	3 859
Drive bogie mass (kg)	2 916	90 %	2 624	125 %	3 645
Primary suspension spring constant (N/m)	465 000	95 %	441 750	125 %	581 250
Primary suspension piled rubber spring constant (N/m)	245 000	85 %	208 250	125 %	306 250
Primary suspension damping constant (Ns/m)	29 400	-	-	-	-
Secondary suspension air spring constant – Inflated (N/m)	360 000	75 %	270 000	150 %	540 000
Secondary suspension air spring damping (Ns/m)	*45 000	-	-	-	-

* Value for secondary suspension air spring damping taken from literature [9]

6.2   *Calibration through optimisation*

In this section, an optimisation technique is used to find those vehicle properties that generate vehicle

eigenfrequencies that most-closely match the dominant frequencies. Cross Entropy (CE) optimisation

is used here to generate a population of trial combinations of the vehicle properties from vector means

and standard deviation. An 'elite set' of well-performing parameters is identified and its mean and

standard deviation used to create a new generation of parameters. The process continues through several

generations until convergence.

In this case, the six parameters influencing the vehicle mass and stiffness matrices are chosen as

variables for the optimisation. Initial mean values, standard deviations, and upper and lower uncertainty

limits for each of the parameters are listed in Table 7. The initial mean value is taken as the stated value

of the property, as indicated on component drawings provided by the train manufacturer (listed in Table

5 Table 6). Initial mean values for the car body and bogie mass moment of inertia, are randomly chosen

values based on typical values found in the literature. Initial values for standard deviation are chosen to

reflect the uncertainty in the stated value of the parameter and are also influenced by its typical order

of magnitude.

Table 7. Vehicle parameters - initial values for mean, standard deviation and range

Vehicle Parameter	Unit	Initial mean (σ)	Initial Standard Deviation (μ)	Lower Limit %	Lower Limit Value	Upper Limit %	Upper Limit Value	Convergence Range ($\pm$)
m_v	kg	38 747	10^3	95 %	36 850	105 %	40 644	50
J_v	kg m^2	611 000	10^5	-	-	-	-	1 000
m_b	kg	3 087	10^3	90 %	2 778	125 %	3 859	25

J_b	kg m²	3 500	10⁴	-	-	-	-	25
k_p	N/m	2 840 000	10⁶	92 %	2 600 000	125 %	3 550 000	5 000
k_s	N/m	720 000	10⁶	75 %	540 000	150 %	1 080 000	5 000

A population of 500 trial solutions are generated for each vehicle parameter using the vector mean and standard deviation. Distributions are truncated within the range of the limits. The parameter values in each trial solution are used to calculate mass and stiffness matrices for the vehicle. A modal analysis is carried out to calculate vehicle eigenfrequencies. An objective function, O, is used to rank each trial solution according to how well they fit to the target frequencies:

$$O = \left(f_{vb} - f_{vb}^{\circ}\right)^2 + \left(f_{vp} - f_{vp}^{\circ}\right)^2 + \left(f_{bb} - f_{bb}^{\circ}\right)^2 + \left(f_{bp} - f_{bp}^{\circ}\right)^2 \qquad (1)$$

where $f_{vb}, f_{vp}, f_{bb}, f_{bp}$ are the eigenfrequencies of the car body bounce, car body pitch, bogie bounce and bogie pitch respectively. Target eigenfrequencies determined in the FDD analysis are denoted with the superscript '°'. The lowest 10% of objective function values are used to define the elite set of vehicle parameters. The elite set is then used to update the vector mean and standard deviation and an updated population of trial values is generated for the next generation. The optimisation technique iterates until the convergence value, C_g, the sum of the differences between consecutive vehicle parameter means, (defined in Equation (2)), falls below a threshold. The convergence threshold value is taken as 1% of the sum of the convergence range values listed in Table 7, in this case, a value of 111.

$$\begin{aligned} C_g = \ & \left|\sigma_{m_v,g} - \sigma_{m_v,g-1}\right| + \left|\sigma_{J_v,g} - \sigma_{J_v,g-1}\right| + \left|\sigma_{m_b,g} - \sigma_{m_b,g-1}\right| + \left|\sigma_{J_b,g} - \sigma_{J_b,g-1}\right| \\ & + \left|\sigma_{k_p,g} - \sigma_{k_p,g-1}\right| + \left|\sigma_{k_s,g} - \sigma_{k_s,g-1}\right| \end{aligned} \qquad (2)$$

where g is the generation number. Following satisfaction of the convergence criterion, the optimisation restarts. This is carried out to ensure that premature convergence to an incorrect solution has not taken place. The population of estimates for the first iteration following a restart is generated using the mean value from the previous iteration and the initial standard deviation. Restarts continue until all vehicle parameters are found consecutively within the convergence range stated in Table 7.

The optimisation is executed 10 times and results are averaged. Table 8 lists the resulting vehicle eigenfrequencies found in each run. The inferred vehicle parameters found in each run are listed in Table 9.

Table 8. Vehicle eigenfrequency targets and results.

Run	Body Bounce $f^{\circ}_{vb} = 1.08$	Body Pitch $f^{\circ}_{vp} = 2.19$	Bogie Bounce $f^{\circ}_{bb} = 6.53$	Bogie Pitch $f^{\circ}_{bp} = 4.31$
1	1.08	2.19	6.53	4.31
2	1.08	2.19	6.53	4.31
3	1.07	2.19	6.53	4.31
4	1.08	2.19	6.53	4.31
5	1.07	2.19	6.53	4.31
6	1.08	2.19	6.53	4.31
7	1.08	2.19	6.53	4.31
8	1.07	2.19	6.53	4.31
9	1.08	2.19	6.53	4.31
10	1.07	2.19	6.53	4.31

Table 9. Optimised vehicle parameter results.

Run	m_v (kg)	J_v (kg m²)	m_b (kg)	J_b (kg m²)	k_p (N/m)	k_s (N/m)
1	36 851	563 743	3 905	9 996	2 771 415	998 708
2	36 852	564 818	3 899	9 972	2 765 009	1 001 119
3	36 851	555 866	3 921	10 075	2 793 281	982 377
4	36 852	563 712	3 925	10 057	2 788 522	997 787
5	36 851	552 341	3 936	10 130	2 808 581	976 691
6	36 853	566 315	3 922	10 039	2 783 245	1 002 765
7	36 853	567 182	3 909	9 991	2 770 168	1 005 658
8	36 851	552 355	3 926	10 106	2 801 895	973 514
9	36 852	567 039	3 905	9 981	2 767 279	1 005 466
10	36 851	556 992	3 923	10 077	2 793 843	983 675
Average	**36 852**	**560 342**	**3 910**	**10 024**	**2 779 145**	**991 748**

In all cases the mass of the car body converges to the minimum allowed by the range. This is at the limit of what would be considered realistic. The mass centre of gravity is assumed to be at the geometrical centre of the rigid bar representing the car body which is unconfirmed in reality and could introduce inaccuracies. Moreover, the mass of the car body is uncertain due to variability in the passenger numbers and fuel loads especially. The distribution of the seated passengers affects the centre of gravity and hence the response of the vehicle. The convergence of this parameter to the limit of its range would suggest that the car body mass is lower than the assumed range. However, this contravenes anecdotal evidence regarding vehicle passenger numbers and fuel loads. This tendency to an unrealistic result may be due to the inaccurate identification of the car body bounce target frequency found through the FDD analysis. This could be solved by improving the design of the band-pass filter so that the power of frequencies close to the cut-off frequency are not lowered significantly to hide a possible alternative car body bounce frequency. An additional sensor installed in the car body would have also been beneficial.

The mass of the bogie increases approximately 20% above its initially stated mass. There are some additional equipment attached to the bogie such as the E-TPWS which would add to the stated mass. However the inferred value for the bogie mass would appear to be greater than expected. This increase in value may also be explained by assumptions made in the numerical modelling of the suspension. Suspension properties in a numerical model are generally considered to be massless and are not considered in the manufacturers' stated mass. Good agreement is found with stated manufacturers' values for primary stiffness. The value for secondary stiffness features the most variation between

restarts. This may be due to the high nonlinearity of this property. Nonetheless, the inferred value is in a range typically used in 2D linear representations of secondary suspension systems found in a number of sources, for example in (Iwnick 1998; Lei and Zhang 2010).

The progression of the optimisation technique through the generations is shown in Figure 10 for 'Run 1'. The population of estimates are represented as a range of dots for each generation. Each heavy black line represents the population mean value for each parameter throughout the 112 generations. It can be seen that there is initially a lot of variability (high standard deviation). As the elite sets are identified and used to generate new generations, the standard deviations tend to reduce.

The sum of the differences between consecutive vehicle parameter means throughout the optimisation for this run is illustrated in Figure 11. To prevent premature convergence, the process is restarted at, for example, generation no. 27. In this run, four restarts are required before the parameter values converge to the criterion required.
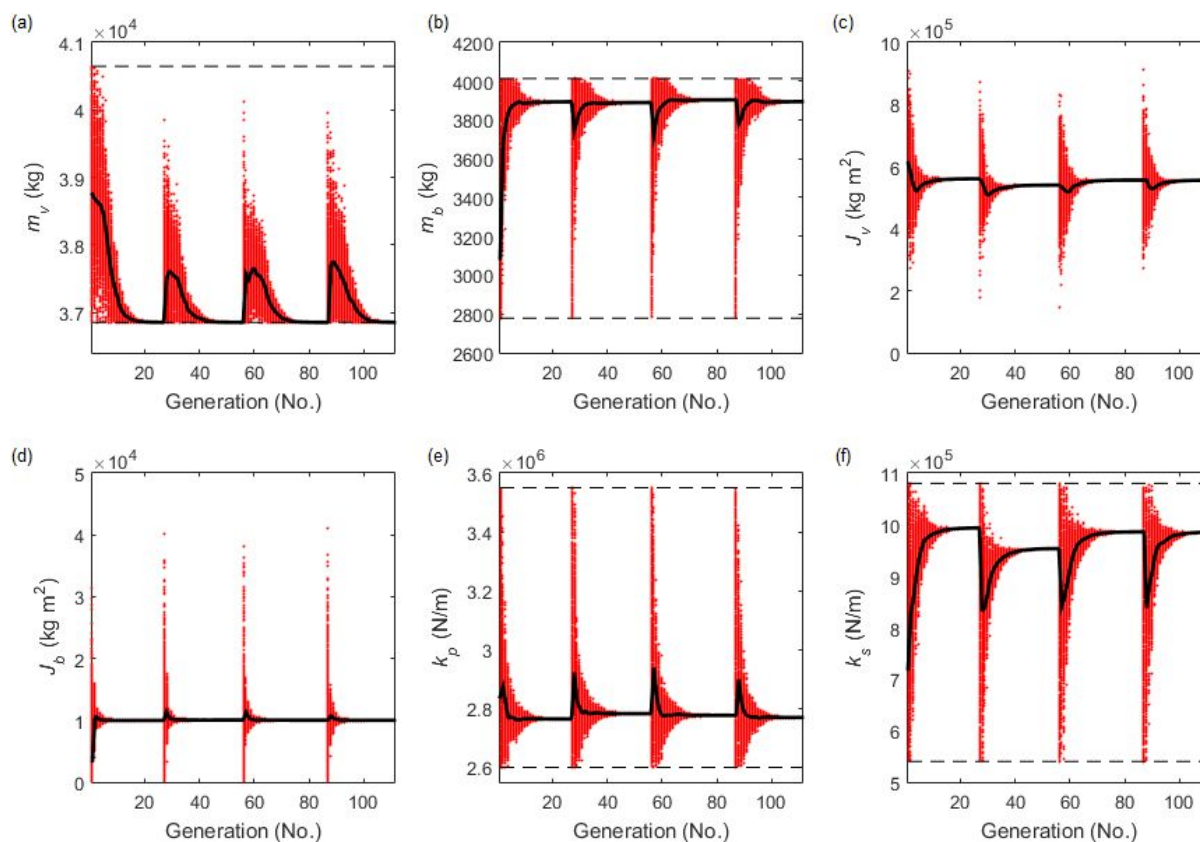

Figure 10. Cross Entropy optimisation for vehicle parameters (Run 1). a) Car body mass; b) Bogie mass; c) Car body mass moment of inertia; d) Bogie mass moment of inertia; e) Primary stiffness; f) Secondary stiffness.
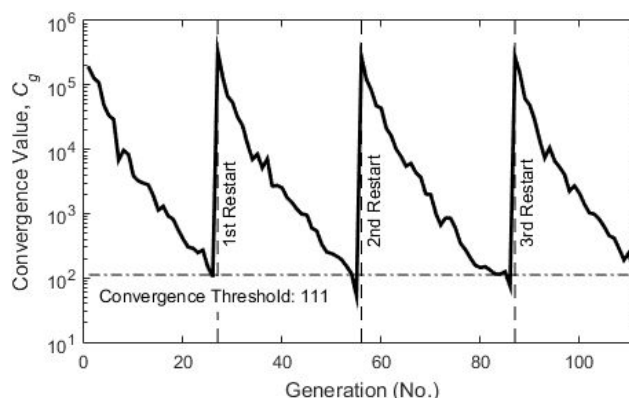
Figure 11. Optimisation convergence value vs generation number (Run 1).

7. VALIDATION TEST ON TRV PROFILE

To access the accuracy of the inferred mechanical properties of the vehicle, this section compares recorded signals to simulated responses. Due to the complexity of railway vehicle dynamics and vehicle-track interaction, it is beneficial to validate the simulation output from the vehicle models against the on-track measurements (Carlbom 2001). A 404 m (quarter-mile) section of track on the Dublin-Belfast railway line was used to verify the numerical response from the calibrated vehicle. This section of track is situated on a straight through a rock cutting and is therefore an area of assumed good subgrade strength. Trains generally travel at full line speed (144 km/h) through the section which is located from 68.54–68.94 km.

The track longitudinal level, shown in Figure 12, was measured by the Irish Rail Track Recording Vehicle (TRV) on the 4th April, 2016. The track longitudinal profile is an average of the left and right longitudinal profile in the D1 wavelength range (3–25 m) measured in accordance with EN13848 (EN13848-1 2003). The profile was measured approximately 2 months after the instrumented train collected data on this railway line; therefore the assumed level of the track at the time of data collection is represented here. According to Irish Rail records, no works were undertaken on this section of line in the time between data collection and measurement by the TRV.
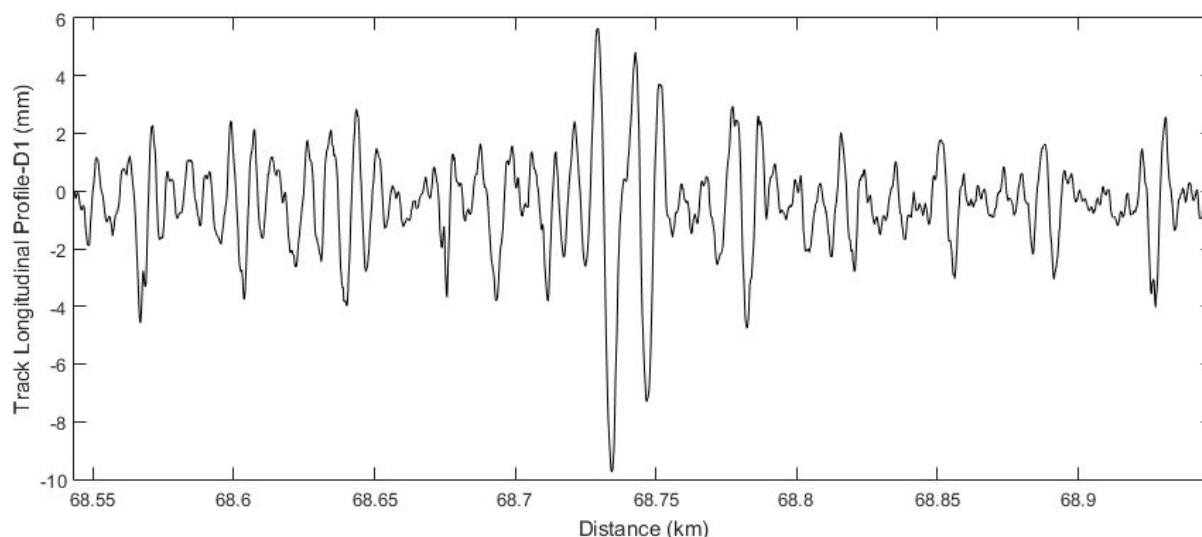
Figure 12. Track Longitudinal Profile (D1) as measured by TRV, 4th April 2016.

The vehicle model is run over this section of track. No track model is considered in the interaction, i.e. the track profile is deemed to be supported by an infinitely stiff track. The average measured train velocity is used as the constant vehicle velocity in the simulation. The bogie vertical acceleration and angular velocity numerical outputs are compared to the actual measured data in Figure 13. A fair match is found between the numerical and measured signals.

The power spectral density plots for the bogie angular velocity and bogie vertical acceleration signals presented in Figure 13 are shown in Figure 14. Only fair agreement is found between the measured and simulated outputs; however there are clearly corresponding peaks of similar magnitude in the 0–10 Hz frequency range for both measurements. The differences between the signal power are larger for the angular velocity which may be a result of inaccuracies arising from the need to apply a sensor calibration factor to the raw data in order to account for the sensor offset.
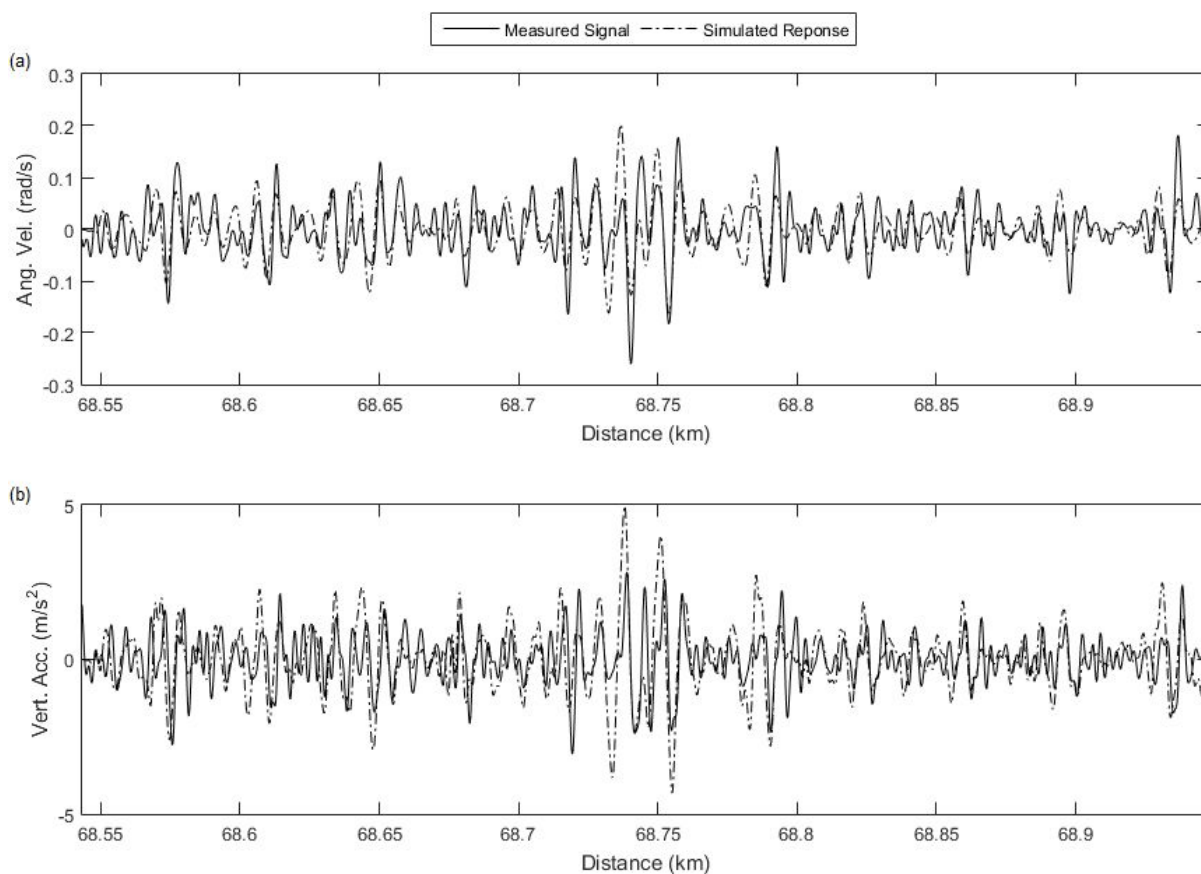
Figure 13. Comparison of measured data and output from calibrated vehicle run over track profile: a) Bogie angular velocity; b) Bogie vertical acceleration.
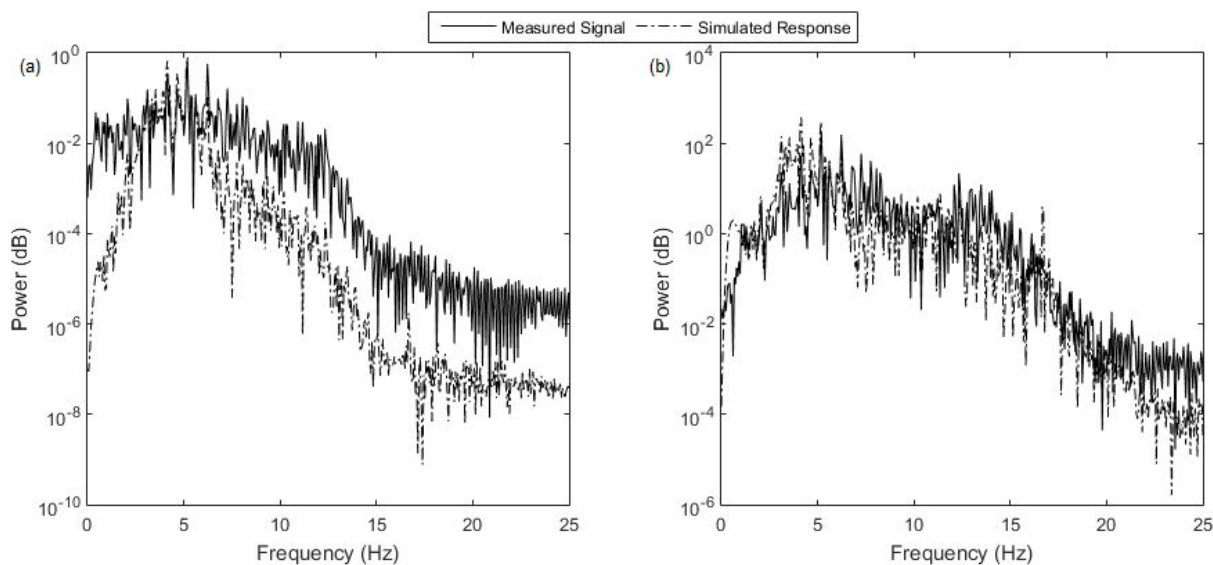

Figure 14. Power spectral density of measured data and output from calibrated vehicle run over track profile; a) Bogie angular velocity, 0–25 Hz; b) Bogie vertical acceleration, 0–25 Hz.

In spite of the fair correlation between the measured vehicle response and the calibrated numerical response within the track section considered, the calibrated vehicle is successfully used to infer track longitudinal profiles. Figure 15 shows a sample result from this work. A track longitudinal profile,

inferred through optimisation from measured vehicle response, is compared to a level survey undertaken on a section of track between 78.0 km and 78.2 km on the Dublin-Belfast railway line.

The optimisation approached proposed by OBrien et al. (2018) is employed here to infer the track profile from the vehicle responses. This is an inverse technique in which the train inertial measurements are used to find the longitudinal track profile that generated the vibration. In this method, CE optimisation is used to find track longitudinal profile from the measured inertial response of the train. A population of trial track longitudinal profiles is generated for both axles on the leading bogie of the vehicle model. Numerical outputs, generated by running the vehicle over the profiles in the population of estimates, are compared to measured data to find an elite set of profiles. This set is used to improve the population of estimates until the method converges to the solution. The details of the process of inferring the track profile from the vehicle responses are given in (OBrien et al. 2018; Quirke et al. 2017). The profiles have been filtered between the wavelengths of 3–25 m. A good estimation of most changes in track level is found however there is a poor match in elevation. This proves that the method has good potential and has benefitted from the calibration exercise described in this paper.
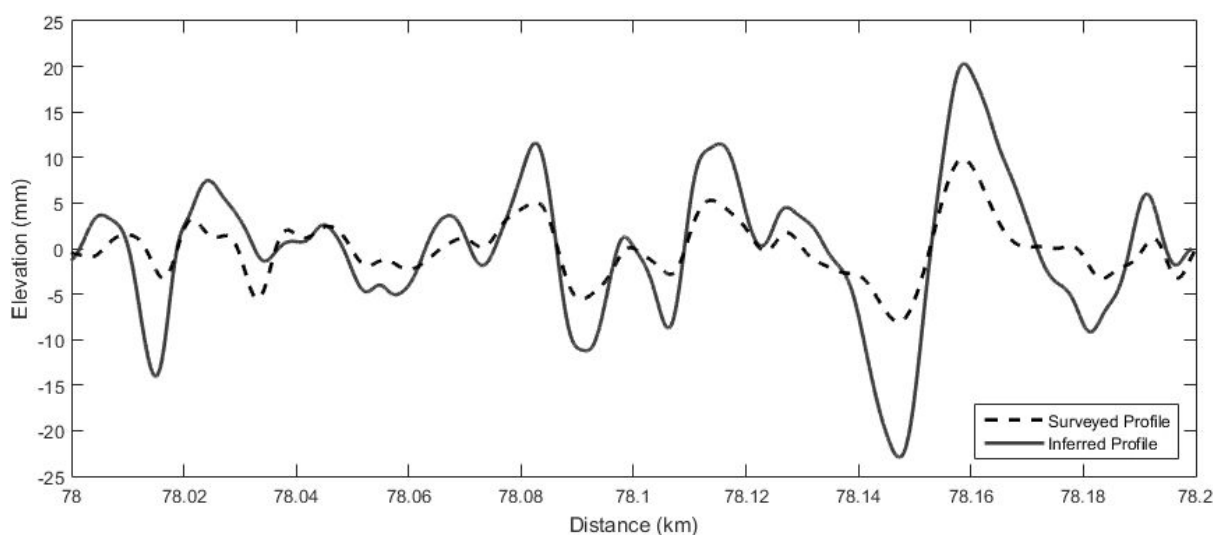

Figure 15. Comparison of track filtered track level survey and filtered inferred track longitudinal profile.

8.   SUMMARY AND CONCLUSIONS

Accurate estimation of vehicle parameters in idealised numerical models is essential for the generation of realistic outputs. In this paper, an experimental calibration of a 2D numerical vehicle model is carried

out to match the measured responses of a railway vehicle. Multiple inertial sensors were installed on an Irish Rail intercity train for a period of 1 month.

Following a filtering process, segmental FDD analysis is used to determine the dominant frequencies common to different datasets from randomly selected segments of data, each 2 km in length. By choosing signals from a number of datasets, the effects of noise, rail profile and other excitations are filtered out and the rigid modes associated with the vehicle dominate.

The vehicle rigid body frequencies identified in this process are used in an optimisation technique to calibrate a 2D rigid body vehicle model. Six parameters are found in the optimisation which matches the numerical vehicle eigenfrequencies to the frequencies found through the FDD analysis. Prior knowledge of some component properties are used as initial values in the optimisation where possible. While inferred values for most parameters are within expected ranges, the car body mass value is unrealistic. This may be due to incorrect identification of its modes of vibration due to limitations on the number of sensors used in the experiment and rigid body modelling assumptions.

Finally the inferred vehicle parameters are chosen as the calibrated vehicle properties. The calibrated vehicle is run over a surveyed track profile. The output from the numerical model is then compared to a sample set of the measured data from the field. A fair match in signal amplitude is found between the model outputs and the measured data. Fair agreement in signal frequency is also found for both signals analysed. The calibrated properties found using this method are used in a technique to find longitudinal track profile from measured vehicle response with encouraging results. This will be the topic of a forthcoming paper.

ACKNOWLEDGEMENT

REFERENCES

Absi, G.N., and Mahadevan, S. 2016. Multi-fidelity approach to dynamics model calibration. Mechanical Systems and Signal Processing, **68-69**: 189-206. doi:10.1016/j.ymssp.2015.07.019.

Ahmadian, H. 2005. Extracting modes of a railway vehicle from measured responces. *In* 1st Int. Oper. Modal Anal. Conf. *Edited by* R. Brincker and N. Møller, Copenhagen, Denmark.

Antolin, P., Zhang, N., Goicolea, J.M., Xia, H., Astiz, M.A., and Oliva, J. 2013. Consideration of nonlinear wheel-rail contact forces for dynamic vehicle-bridge interaction in high-speed railways. Journal of Sound and Vibration, **332**(5): 1231-1251. doi:10.1016/j.jsv.2012.10.022.

Azimi, H. 2011. Development of VBI models with vehicle acceleration for bridge-vehicle dynamic response. Concordia University, Canada.

Brincker, R., Zhang, L.M., and Andersen, P. 2001. Modal identification of output-only systems using frequency domain decomposition. Smart Materials & Structures, **10**(3): 441-445. doi:Doi 10.1088/0964-1726/10/3/303.

Carlbom, P.F. 2001. Combining MBS with FEM for rail vehicle dynamics analysis. Multibody System Dynamics, **6**(3): 291-300. doi:Doi 10.1023/A:1012072405882.

De Rosa, A., Alfi, S., and Bruni, S. 2019. Estimation of lateral and cross alignment in a railway track based on vehicle dynamics measurements. Mechanical Systems and Signal Processing, **116**: 606-623.

Diana, G., Cheli, F., Collina, A., Corradi, R., and Melzi, S. 2002. The development of a numerical model for railway vehicles comfort assessment through comparison with experimental measurements. Vehicle System Dynamics, **38**(3): 165-183. doi:DOI 10.1076/vesd.38.3.165.8287.

Domenech, A., Museros, P., and Martinez-Rodrigo, M.D. 2014. Influence of the vehicle model on the prediction of the maximum bending response of simply-supported bridges under high-speed railway traffic. Engineering Structures, **72**: 123-139. doi:10.1016/j.engstruct.2014.04.037.

EN13848-1. 2003. Railway Applications - Track - Track Geometry Quality - Part 1: Characterisation of track geometry. *In* CEN.

Ferrara, R. 2013. A numerical model to predict train induced vibrations and dynamic overloads. University of Reggio Calabria, Italy.

Francois, S., Galvin, P., Schevenels, M., Lombaert, G., and Degrande, G. 2012. A 2.5D Coupled FE-BE Methodology for the Prediction of Railway Induced Vibrations. Noise and Vibration Mitigation for Rail Transportation Systems, **118**: 367-374. Available from <Go to ISI>://WOS:000307422700043 [accessed.

Iwnick, S. 1998. Manchester benchmarks for rail vehicle simulation. Vehicle System Dynamics, **30**(3-4): 295-313. doi:Doi 10.1080/00423119808969454.

Kouroussis, G., and Verlinden, O. 2013. Prediction of railway induced ground vibration through multibody and finite element modelling. Mechanical Sciences, **4**(1): 167-183. doi:10.5194/ms-4-167-2013.

Kouroussis, G., Verlinden, O., and Conti, C. 2011. Free field vibrations caused by high-speed lines: Measurement and time domain simulation. Soil Dynamics and Earthquake Engineering, **31**(4): 692-707. doi:10.1016/j.soildyn.2010.11.012.

L. Zhang, R. Brincker, and Andersen, P. 2005. An overview of operational modal analysis: major development and issues. *In* 1st Int. Oper. Modal Anal. Conf. *Edited by* R. Brincker and N. Møller, Copenhagen, Denmark.

Lei, X., and Noda, N.A. 2002. Analyses of dynamic response of vehicle and track coupling system with random irregularity of track vertical profile. Journal of Sound and Vibration, **258**(1): 147-165. doi:10.1006/jsvi.2002.5107.

Lei, X., and Zhang, B. 2010. Influence of track stiffness distribution on vehicle and track interactions in track transition. Proceedings of the Institution of Mechanical Engineers Part F-Journal of Rail and Rapid Transit, **224**(F6): 592-604. doi:10.1243/09544097jrrt318.

Li, P., Goodall, R., Weston, P., Ling, C.S., Goodman, C., and Roberts, C. 2007. Estimation of railway vehicle suspension parameters for condition monitoring. Control Engineering Practice, **15**(1): 43-55. doi:10.1016/j.conengprac.2006.02.021.

Lin, C.C., Wang, J.F., and Chen, B.L. 2005. Train-Induced Vibration Control of High-Speed Railway Bridges Equipped with Multiple Tuned Mass Dampers. Journal of Bridge Engineering, **10**(4): 398-414. doi:10.1061/(Asce)1084-0702(2005)10:4(398).

Lin, Y.H., and Trethewey, M.W. 1990. Finite-Element Analysis of Elastic Beams Subjected to Moving Dynamic Loads. Journal of Sound and Vibration, **136**(2): 323-342. doi:Doi 10.1016/0022-460x(90)90860-3.

Liu, K., Reynders, E., De Roeck, G., and Lombaert, G. 2009. Experimental and numerical analysis of a composite bridge for high-speed trains. Journal of Sound and Vibration, **320**(1-2): 201-220. doi:10.1016/j.jsv.2008.07.010.

Lou, P. 2007. Finite element analysis for train-track-bridge interaction system. Archive of Applied Mechanics, **77**(10): 707-728. doi:10.1007/s00419-007-0122-4.

Malekjafarian, A., and OBrien, E.J. 2014. Identification of bridge mode shapes using Short Time Frequency Domain Decomposition of the responses measured in a passing vehicle. Engineering Structures, **81**: 386-397. doi:10.1016/j.engstruct.2014.10.007.

Malekjafarian, A., OBrien, E.J., and Cantero, D. Railway track monitoring using drive-by measurements. *In* The Fifteenth East Asia-Pacific Conference on Structural Engineering and Construction (EASEC-15), Xi'an, China, 11-13 October 2017. 2017.

Malekjafarian, A., OBrien, E., Quirke, P., and Bowe, C. 2019. Railway Track Monitoring Using Train Measurements: An Experimental Case Study. Applied Sciences, **9**(22): 4859.

Mottershead, J.E., and Friswell, M.I. 1993. Model Updating in Structural Dynamics - a Survey. Journal of Sound and Vibration, **167**(2): 347-375. doi:DOI 10.1006/jsvi.1993.1340.

Nguyen, K., Goicolea, J.M., and Galbadon, F. 2014. Comparison of dynamic effects of high-speed traffic load on ballasted track using a simplified two-dimensional and full three-dimensional model. Proceedings of the Institution of Mechanical Engineers Part F-Journal of Rail and Rapid Transit, **228**(2): 128-142. doi:10.1177/0954409712465710.

OBrien, E.J., Bowe, C., Quirke, P., and Cantero, D. 2017. Determination of longitudinal profile of railway track using vehicle-based inertial readings. Proceedings of the Institution of Mechanical Engineers Part F-Journal of Rail and Rapid Transit, **231**(5): 518-534. doi:10.1177/0954409716664936.

OBrien, E.J., Quirke, P., Bowe, C., and Cantero, D. 2018. Determination of railway track longitudinal profile using measured inertial response of an in-service railway vehicle. Structural Health Monitoring, **17**(6): 1425-1440.

Quirke, P. 2017. Drive-by detection of railway track longitudinal profile, stiffness and bridge damage. University College Dublin.

Quirke, P., Bowe, C., OBrien, E.J., Cantero, D., Antolin, P., and Goicolea, J.M. 2017. Railway bridge damage detection using vehicle-based inertial measurements and apparent profile. Engineering Structures, **153**: 421-442.

Ribeiro, D., Calcada, R., Delgado, R., Brehm, M., and Zabel, V. 2013. Finite-element model calibration of a railway vehicle based on experimental modal parameters. Vehicle System Dynamics, **51**(6): 821-856. doi:10.1080/00423114.2013.778416.

Rubinstein, R.Y., and Kroese, D.P. 2013. The cross-entropy method: a unified approach to combinatorial optimization, Monte-Carlo simulation and machine learning. Springer Science & Business Media.

S. Popprath, C. Benatzky, C. Bilik, M. Kozek, A. Stribersky, and Wassermann, J. 2006. Experimental modal analysis of a scaled car body for metro vehicles. *In* 13th Int. Congr. Sound Vib., Vienna, Austria.

Stribersky, A., Moser, F., and Rulka, W. 2002. Structural dynamics and ride comfort of a rail vehicle system. Advances in Engineering Software, **33**(7-10): 541-552. doi:Doi 10.1016/S0965-9978(02)00072-8.

Sun, Y.Q., and Dhanasekar, M. 2002. A dynamic model for the vertical interaction of the rail track and wagon system. International Journal of Solids and Structures, **39**(5): 1337-1359. Available from <Go to ISI>://WOS:000174896100014 [accessed.

Weston, P., Roberts, C., Yeo, G., and Stewart, E. 2015. Perspectives on railway track geometry condition monitoring from in-service railway vehicles. Vehicle System Dynamics, **53**(7): 1063-1091. doi:10.1080/00423114.2015.1034730.

Xiao, X., Sun, Z., and Shen, W. 2020. A Kalman filter algorithm for identifying track irregularities of railway bridges using vehicle dynamic responses. Mechanical Systems and Signal Processing, **138**: 106582.

Xu, L., and Zhai, W. 2019a. A three-dimensional model for train-track-bridge dynamic interactions with hypothesis of wheel-rail rigid contact. Mechanical Systems and Signal Processing, **132**: 471-489.

Xu, L., and Zhai, W. 2019b. A three-dimensional dynamic model for train-track interactions. Applied Mathematical Modelling, **76**: 443-465.

Xu, L., Yu, Z., and Shi, C. 2020. A matrix coupled model for vehicle-slab track-subgrade interactions at 3-D space. Soil Dynamics and Earthquake Engineering, **128**: 105894.

Zhai, W., Wang, S., Zhang, N., Gao, M., Xia, H., Cai, C., and Zhao, C. 2013a. High-speed train–track–bridge dynamic interactions–Part II: experimental validation and engineering application. International Journal of Rail Transportation, **1**(1-2): 25-41.

Zhai, W., Xia, H., Cai, C., Gao, M., Li, X., Guo, X., Zhang, N., and Wang, K. 2013b. High-speed train–track–bridge dynamic interactions–Part I: theoretical model and numerical simulation. International Journal of Rail Transportation, **1**(1-2): 3-24.

Zhai, W.M., Wang, K.Y., and Cai, C.B. 2009. Fundamentals of vehicle-track coupled dynamics. Vehicle System Dynamics, **47**(11): 1349-1376. doi:10.1080/00423110802621561.

Figures:

Figure 16. The research gap addressed in this paper.

Figure 17. 2D Car model.

Figure 18. Sensor installation locations on trailer bogie (dimensions in mm). (CAD drawing sourced from Tokyu Car Corporation).

Figure 19. a) Bogie mounted gyrometer and accelerometer; b) Uniaxial accelerometer clamped to axle box; c) Data logger (HBM Somat eDAQ lite) housed in disused train coupler box in close proximity to sensors

Figure 20. Bogie angular velocity signal (pitch velocity) as a function of distance from the start point (Dublin); a) Unfiltered signal; b) Band-pass filtered signal (0.25-25 Hz)

Figure 21. Bogie vertical acceleration signal as a function of distance from the start point (Dublin); a) Unfiltered signal; b) Band-pass filtered signal (0.25-25 Hz)

Figure 22. Power spectral density of captured signals. a) Bogie angular velocity 0–100 Hz; b) Bogie vertical acceleration 0–100 Hz; c) Detailed view of bogie vertical acceleration 45–60 Hz.

Figure 23. FDD Methodology; a) Traditional FDD: data sampled over same time period from a number of channels; b) Segmental FDD: data sampled randomly from multiple datasets, in this case multiple train trips.

Figure 24. Sum of singular values from FDD analysis of 30 datasets (2 km signal segments). a) Axle 1 vertical acceleration; b) Axle 2 vertical acceleration; c) Bogie vertical acceleration; d) Bogie angular velocity.

Figure 25. Cross Entropy optimisation for vehicle parameters (Run 1). a) Car body mass; b) Bogie mass; c) Car body mass moment of inertia; d) Bogie mass moment of inertia; e) Primary stiffness; f) Secondary stiffness.

Figure 26. Optimisation convergence value vs generation number (Run 1).

Figure 27. Track Longitudinal Profile (D1) as measured by TRV, 4th April 2016.

Figure 28. Comparison of measured data and output from calibrated vehicle run over track profile: a) Bogie angular velocity; b) Bogie vertical acceleration.

Figure 29. Power spectral density of measured data and output from calibrated vehicle run over track profile; a) Bogie angular velocity, 0–25 Hz; b) Bogie vertical acceleration, 0–25 Hz.

Figure 30. Comparison of track filtered track level survey and filtered inferred track longitudinal profile.